Polarization-mixing optical parametric oscillator

Gal Kalmani and Ady Arie

Department of Physical Electronics, Tel-Aviv University, Tel-Aviv 69978, Israel

Pinhas Blau and Shaul Pearl

Electro Optics Division, Soreg NRC, Yavne 81800, Israel

Arlee V. Smith

Sandia National Laboratories, Albuquerque, New Mexico 87185-1423

Received March 8, 2005

We report the experimental realization of a new type of optical parametric oscillator in which oscillation is achieved by polarization rotation in a linear retarder, followed by nonlinear polarization mixing. The mixing is performed by a type II degenerate parametric downconversion in a periodically poled KTP crystal pumped by a 1064 nm pulsed Nd:YAG pump. A single, linearly polarized beam, precisely at the degenerate wavelength is generated. The output spectrum has a narrow linewidth (below the instrumentation bandwidth of 1 nm) and is highly stable with respect to variations in the crystal temperature. © 2005 Optical Society of America

OCIS codes: 190.4970, 190.4360.

Quasi-phase-matched frequency conversion using periodically poled crystals has proved to be a mature technology for generating coherent light where conventional lasers are unavailable. Optical parametric generation was thoroughly investigated and implemented in various configurations and devices. A special case of an optical parametric oscillator (OPO) is the degenerate OPO, where both the signal and the idler wavelengths are at twice the pump wavelength. A type I phase-matched degenerate OPO is characterized by a broad spectral bandwidth, which limits the usefulness of its output beam. Type II phasematched degenerate interaction results in narrow bandwidth, yet at this configuration the signal and idler beams are generated at two orthogonal polarizations. In both type I and type II interactions, the bandwidth is highly sensitive to crystal temperature due to the temperature dependence of the refractive indices. Fifteen years ago, Guyer and Lowenthal² suggested a new configuration in which the orthogonally polarized signal and idler beams that are generated in a type II phase-matched degenerate interaction are mixed using an intracavity linear retarder. A linear output polarization is enforced by an intracavity polarizer. A similar polarization-mixing approach (but without the intracavity polarizer) was used by Mason and Wong³ to demonstrate self-phase locking of the signal and idler continuous waves in a degenerate type II OPO.

The polarization-mixing approach may provide a single, linearly polarized beam with narrow linewidth at the degenerate point. In this configuration, a type II degenerate parametric downconversion process generates two waves with identical wavelengths and orthogonal polarizations. In each round trip, one of these waves is coupled out of the cavity, whereas the other is rotated by 90° with a linear retarder. As a result, in the next round trip, this remaining wave will also be coupled out of the cavity, but before that it will mix with the pump in the nonlinear crystal to

generate a new orthogonally polarized wave, which will remain for the next round trip, etc. The motivation for our research was to demonstrate a degenerate pulsed OPO that produces a single, linearly polarized beam and exhibits a narrow and stable linewidth. To the best of our knowledge, this polarization-mixing oscillator (PMO) configuration has never been realized.

Figure 1 illustrates the PMO configuration that we implemented. The 65 mm long hemispherical cavity consisted of a periodically poled KTP (PPKTP) crystal with a period of $\Lambda=60~\mu m$ for quasi-phase-matching a degenerate type II interaction from 1064 to 2128 nm. ^{4,5} The 36 mm long, 2 mm thick, and 10 mm wide crystal was polished and antireflection coated on both sides for the pump and signal waves. The phase-matching temperature for degenerate downconversion was 70°C. The cavity input mirror was >99% transmitting at the pump wavelength and 99% reflecting at around 2.128 μm , whereas the rear OPO mirror was highly reflecting at both wavelengths. The pump waist on the rear OPO mirror was ~100 μm . A specially designed wave plate, which has

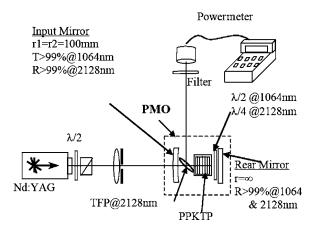


Fig. 1. PMO experimental setup.

a quarter-wave retardation at 2.13 μm and a half-wave retardation at 1.064 μm , was inserted between the nonlinear crystal and the rear OPO mirror. When the signal and idler were double passed through this retarder, the polarizations were interchanged. A thin-film Brewster polarizer (TFP) with an extinction ratio of 1:100 for the transmitted beam was inserted between the input OPO mirror and the nonlinear crystal and coupled the Z-polarized wave out of the cavity while transmitting the Y-polarized wave at both signal and pump wavelengths. The cavity round-trip losses for the Y-polarized signal were $\sim 10\%$.

The multilongitudinal-mode pump source was a Spectra-Physics electro-optically Nd:YAG laser, Model X30-106Q, operating at 1 kHz with a 28 ns pulse width and a beam quality of 1.1 times the diffraction limit. A half-wave plate and a polarizer enabled rotation of the Z-polarized laser light into the Y direction to vary its output energy from 0 to the maximum of 1.4 mJ/pulse. A bandpass filter around 2 μ m and a powermeter were used to measure the output beam power. As shown in Fig. 2, the threshold pump power was 380 mW, and 300 mW of output power was obtained at a 1.35 W pump. Light-to-light efficiency was over 22% with a slope efficiency above 30%. The corresponding threshold intensity was 34 MW/cm², which is in very good agreement with two theoretical estimates, one based on a plane-wave analysis and the other based on numeric SNLO⁶ simulation, as outlined below. The nonlinear coefficient in the simulation was assumed to be 2.3 pm/V [=2/ $\pi \times d_{24}$ (Ref. 7)].

We measured the PMO's output spectrum with a monochromator. The PMO linewidth was found to be even narrower than that of a conventional type II doubly resonating OPO (DRO). In a DRO configuration with the same crystal, we demonstrated a spectral linewidth of 2 nm. In the PMO, the spectral linewidth was below the 1 nm monochromator instrumentation limit. Figure 3 presents a comparison of the output spectra of three OPO configurations: a degenerate type I DRO (using the suitable PPKTP crystal), a degenerate type II DRO, and our degenerate type II PMO. In contrast with the type II

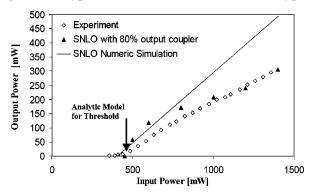


Fig. 2. Output power versus input pump power for the PMO. Diamonds, experimental results; solid line, triangles—results based on SNLO simulation with 100% and 80% output coupling, respectively; arrow, threshold calculated using Eq. (2).

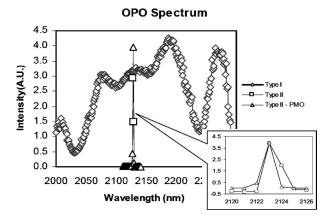


Fig. 3. Comparison of the spectrum of degenerate type I and type II DROs and a degenerate PMO. Inset, spectra of the type II DRO and the PMO with an expanded wavelength scale.

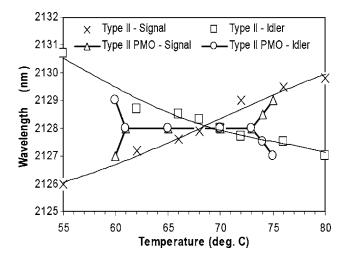


Fig. 4. Oscillation wavelengths as a function of crystal temperature in a type II DRO and PMO.

DRO and PMO, the type I OPO generates a very wide linewidth of more than 300 nm.

Figure 4 shows the dependence of the PMO output wavelength on the crystal temperature. Although conventional type II DRO exhibits a narrow linewidth, as the crystal temperature is varied from the degenerate temperature, the idler and signal wavelengths are no longer the same and thus the spectral linewidth is broadened. In contrast, the PMO output wavelength is nearly independent of the crystal temperature. The device stays at degeneracy even though the crystal temperature was changed over 12°C. This is a unique feature that is due to the polarization-mixing process of the device, which locks signal and idler wavelengths at the degenerate point. In a standard OPO, a nondegenerate pair of the signal and idler wavelengths exhibits higher gain when the crystal temperature is changed, thereby causing the OPO to shift from the degeneracy point. In contrast, in a PMO, this nondegenerate pair may be phase matched in one propagation direction, but it is out of phase matching in the opposite propagation direction owing to the polarization interchange in the retarder. The degenerate pair is not precisely phase

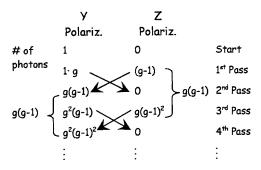


Fig. 5. Photon flux evolution at the PMO.

matched in both directions, but our simulations show that its overall gain still remains higher than that of the nondegenerate pair. Further increase (or decrease) in the crystal temperature leads to splitting of the PMO output into two wavelengths. This may be caused by the wavelength dependence of the retarder and polarizer inside the PMO, which do not completely suppress wavelengths that are different from the degenerate wavelength.

Figure 5 demonstrates the evolution of the generated photon flux in the PMO. Each line in the table relates to the photon number after a single-pass amplification in the nonlinear crystal. The odd and even lines relate to propagation in opposite directions in the cavity. At each odd pass, the *Y*-polarized beam is amplified by a factor of g, and the same number of photons is generated at the orthogonal (*Z*-polarized) beam. After a complete round trip in the cavity the Zand Y-polarized beams are exchanged, and the Z-polarized beam is coupled out through the polarizer. The total round-trip gain is g(g-1). The singlepass signal power gain, using the square gain model.8 is $g = e^{-2\alpha l} \cosh^2(\Gamma l)$, where α is the absorption coefficient, l is the crystal length, and Γ is the parametric amplitude gain coefficient. For a pump pulse length auand cavity length L, the number of round trips per pulse is $p = c\tau/2L$ and the PMO gain is given by

$$\frac{P_n}{P_0} = [Rg(g-1)]^p \approx \{\text{Re}^{-4\alpha l} [\cosh^2(\Gamma l)] [\cosh^2(\Gamma l) - 1]\}^p,$$
(1)

where R is the cavity mirror reflectivity and P_n and P_0 are the threshold and noise powers, respectively. Equation (1) is solved analytically to get the PMO's threshold intensity:

$$\begin{split} I_{Th} &= \frac{n_s n_i n_p \varepsilon_0 c^3}{2 \omega_s \omega_i g_s d_{eff}^2} \left(\frac{1.34}{l}\right)^2 \\ &\times \left[\cosh^{-1} \left(\frac{1}{\sqrt{2}} \sqrt{1 + \sqrt{1 + \frac{4}{\text{Re}^{-4\alpha l}} \left(\frac{P_n}{P_0}\right)^{2L/c\tau}}}\right)\right]^2, \end{split} \tag{2}$$

where n_s , n_i , and n_p are the signal, idler, and pump

refractive indices, respectively; ω_s and ω_i are the signal and idler angular frequencies, respectively; and g_s is the mode coupling coefficient. Using the same criteria for P_n/P_0 at threshold as in Ref. 8, i.e., $\ln(P_n/P_0)=33$, the threshold value is 39 MW/cm², which is in good agreement with the experimentally measured threshold of 34 MW/cm². For comparison, the threshold intensity of a standard singly resonant double-pass-pumped OPO with the same cavity loss and nonlinearity is 24 MW/cm².

The PMO interaction was also simulated numerically using the SNLO nonlinear optics code⁶ with the single-frequency two-dimensional OPO model. A special module was developed to simulate the PMO configuration. The simulation results, which take into account the values of the PMO cavity elements, are also presented in Fig. 2. If we assume perfect 100% output coupling through the TFP, the simulation predicts higher slope efficiency than what we measured. The experimental results may be explained by assuming lower output coupling of 80%. The exact coupling ratio could not be measured owing to the tight placement of elements in the PMO.

In summary, a new OPO configuration was experimentally demonstrated. This PMO emits a single, linearly polarized beam with a narrow spectral width of less than 1 nm at the degenerate wavelength. This is due to the nonlinear mixing of the two type II orthogonal polarizations. The emission wavelength is fixed at 2128 nm independent of the crystal temperature over $\Delta T = 12$ °C. More than 300 mW of polarized output power and 22% light-to-light efficiency were obtained. The narrow and stable spectral linewidth makes this device an attractive candidate for pumping another OPO toward the mid-infrared spectral range or to be used as a seeder for a type I degenerate optical parametric amplifier. The PMO may also be used in continuous-wave operation as a frequency divider³ in a frequency chain for precision spectral measurements.

We thank Moti Katz from Soreq NRC for fabricating the PPKTP crystals that were used in this research. A. Arie's e-mail address is ady@eng.tau.ac.il.

References

- R. L. Byer, J. Nonlinear Opt. Phys. Mater. 6, 549 (1997).
- R. D. Guyer and D. D. Lowenthal, Proc. SPIE 1220, 41 (1990).
- 3. E. J. Mason and N. C. Wong, Opt. Lett. **23**, 1733 (1998).
- M. Katz, D. Eger, M. B. Oron, and A. Hardy, J. Appl. Phys. 90, 53 (2001).
- M. Katz, D. Eger, M. B. Oron, and A. Hardy, J. Appl. Phys. 92, 7702 (2002).
- A. V. Smith, "SNLO nonlinear optics code," Sandia National Laboratories, Albuquerque, N.M. 87185-1423 (2004).
- 7. R. W. Boyd, Nonlinear Optics, 2nd ed. (Academic 2003).
- S. J. Brosnan and R. L. Byer, IEEE J. Quantum Electron. QE-15, 415 (1979).